Available online at www.sciencedirect.com
SCIENCE DIRECT®
Journal of Organometallic Chemistry 690 (2005) 773–783
Journal of Organometallic Chemistry
www.elsevier.com/locate/jorganchem

Polymerization of ethene with zirconocene catalysts: an experimental and quantum chemical study of the influence of *para*-substituent in benzyl in bis{η^5-(1-benzyl)indenyl}zirconium dichlorides

Erkki Aitola *, Marina Surakka [1], Timo Repo *, Mikko Linnolahti [2], Kristian Lappalainen, Kaisa Kervinen, Martti Klinga, Tapani Pakkanen [2], Markku Leskelä

Laboratory of Inorganic Chemistry, Department of Chemistry, University of Helsinki, P.O. Box 55, FIN-00014 Helsinki, Finland

Received 17 February 2004; accepted 6 September 2004
Available online 8 December 2004

Abstract

The *meso*- and *rac*-like isomers of bis{η^5-(1-benzyl)indenyl}zirconium dichloride (**5**), bis{η^5-(1-*para*-methoxybenzyl)indenyl}zirconium dichloride (**6**), bis{η^5-(1-*para*-fluoro-benzyl)indenyl}zirconium dichloride (**7**) and bis{η^5-(1-phenylethyl)indenyl}zirconium dichloride (**8**) were synthesized and isolated. Solid-state structures of *meso*- and *rac*-like **5** were determined by X-ray structure analysis. Polymerization properties of the methylaluminoxane (MAO) activated diastereomers of complexes **5**–**8** were studied in ethene polymerizations under different monomer concentrations. The *rac*-like isomer of 1-phenylethyl-substituted **8**/MAO showed significantly higher activity than the 1-benzyl substituted analogs **5**–**7**/MAO. In addition, *rac*-**8**/MAO behaves like a single center catalyst producing polyethene with narrow molar mass distribution (1.8–1.9), while diastereomers of **5**–**7**/MAO produce polymers with molar mass distributions varying from 2.7 up to 10.3. The *rac* and *meso*-like isomers of **5**–**7**/MAO have different response on the monomer concentration. Quantum chemical calculations suggest a strong interaction between the benzyl substituent and the electron deficient zirconium center. The phenyl metal coordination energies depend on the electronic properties of the *para*-substituent. In **8**/MAO, due to the ethyl spacer, the coordination does not have a significant role and therefore much higher activity and single center polymerization behavior is observed.

1. Introduction

Metallocene dichlorides activated with methylaluminoxanes (MAO) are highly active catalyst for the polymerization of α-olefins [1]. Unlike traditional heterogeneous Ziegler–Natta catalysts, *single center* metallocenes provide precise control to polymer syntheses, allowing the preparation of polymers with well-defined microstructures. Olefin polymerization with metallocene catalysts obeys well-defined kinetics and polymers prepared have low molar mass distribution [2]. The basic, sterically open unbridged metallocene, bis(η^5-cyclopentadienyl)zirconium-dichloride, Cp_2ZrCl_2, polymerizes ethene to linear high molar mass crystalline polyethene with good activity [3]. A variety of metallocene dichloride precursors with different cyclopentadienyl (Cp) and indenyl (Ind) ligand modifications have been developed to improve the activity or to control the monomer insertion process or both [4].

* Corresponding authors. Tel.: +35 85 055 78048; fax: +35 89 191 50198.
E-mail address: erkki.aitola@helsinki.fi (E. Aitola).
[1] Present address: Borealis Polymers Oy, P.O. Box 330, FIN-06101 Porvoo, Finland.
[2] Department of Chemistry, University of Joensuu, P.O. Box, 111 FIN-80101 Joensuu, Finland.

0022-328X/$ - see front matter © 2004 Elsevier B.V. All rights reserved.
doi:10.1016/j.jorganchem.2004.09.089

The function of different substitution patterns of the Cp- or Ind-ring is to create an electronically and sterically optimized surrounding for the catalytic active metal center. The size and symmetry of substituents linked to the Cp or Ind moieties are essential variables for tuning the polymerization efficiency of catalysts and polymer properties. Benzyl substitution of the ligands is an interesting way to sterically and electronically modify the chemical structure of the catalyst as interactions between a phenyl ring and the transition metal center in metallocenes can occur [5,6]. Computational studies of benzyl-substituted $[(\eta^5\text{-Cp})(\eta^5\text{-CpCH}_2\text{C}_6\text{H}_5)]\text{ZrMe}^+$ have shown that η^3- and η^1-coordination modes of ring carbons are energetically more favorable than an agostic interaction via hydrogen [7].

In our earlier studies, *rac*- and *meso*-like [8] isomers of the unbridged bis{(*para*-fluoro-indenyl)}$ZrCl_2$ (**7**) showed moderate activity in ethene polymerization but lacked the capability to polymerize propene [9]. In augmentation for this study we investigated various ligand systems where the *para*-substituent attached to the benzyl group was varied. Here we report synthesis of a series of benzyl-substituted bis(1-indenyl) zirconocene dichlorides, use of their separated *rac* and *meso* forms in ethene polymerization and quantum chemical studies to illustrate interactions between various benzyl moieties and the cationic metal center.

2. Results

2.1. Synthesis of ligands and complexes

Indene derivatives having a benzyl substituent in 1-position are easily synthesized by reacting indenyl lithium with appropriate benzyl halides in polar solvents [9,10]. After the reaction, ligand precursors were purified by column chromatography and isolated with moderate to good yields. Treatment of $ZrCl_4$ with lithio salts of the ligand precursors **1**–**4** in dichloromethane gave the complexes **5**–**8** with 1:1 mixture of *rac*/*meso* isomers (Scheme 1). Different solubilities of the *rac* and *meso* isomers allowed separation of the diastereomers under carefully chosen crystallization conditions. Crystals of both isomers of complex **5** suitable for X-ray diffraction measurements were obtained by this manner.

In the ^{1}H NMR spectrum the chemical shifts of the indenyl five-member ring and the CH_2 linkage of the benzyl group are slightly affected by the different substituents in the phenyl moiety. A methoxy substituent in *para*-position (**6**) moves the signals to higher field while the electron-withdrawing *p*-fluoro substituent (**7**) moves them to lower field compared to the signals found for the unsubstituted benzyl unit (**5**). In the ^{1}H NMR spectra the difference in chemical shifts of the *rac* and *meso* isomers of **5**–**8** can be clearly distinguished by the appearing of the protons of indenyl five-member ring. In complex **6**, for example, these peaks appear at 5.22 and 6.20 ppm for the *meso* form and at 5.73 and 5.97 ppm for the *rac* isomer. There are also slight differences in the shifts of the CH_2 linkage protons for two isomers; the signals appear at slightly higher field for the *rac* isomers.

2.2. Solid-state structures of meso- and rac-5

The Ortep illustrations of the crystal structures of *meso*-**7**, *meso*-**5** and *rac*-**5** are presented in Fig. 1. In the solid-state *meso*-**5** is C_1-symmetric and the geometry around the Zr center differs only slightly from that of *meso*-**7** [9]. *meso*-**5** crystallizes in a central/lateral *gauche*-type orientation just like the *meso*-**7** while *rac*-**5** crystallizes in a bis-lateral *anti*-type orientation similar as reported for bis{(1-cyclohexyl)tetrahydroindenyl}$ZrCl_2$ [11]. In *rac*-**5** the ligands are symmetry equivalent and the complex is C_2-symmetric. The bond distances between Zr–Cl and Zr–Cp both in *meso*- and *rac*-**5** (Table 1) correspond to the distances reported

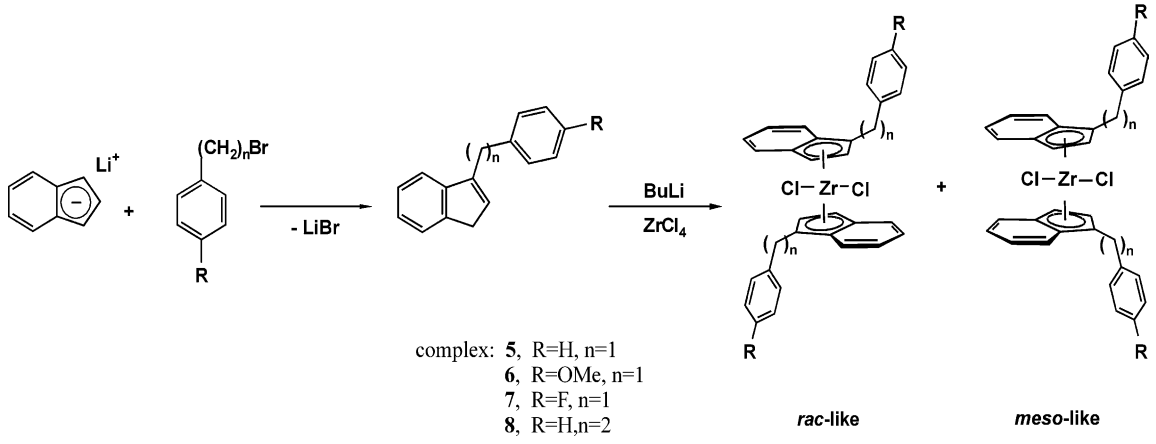

Scheme 1. Synthesis of ligands **1**–**4** and complexes **5**–**8**.

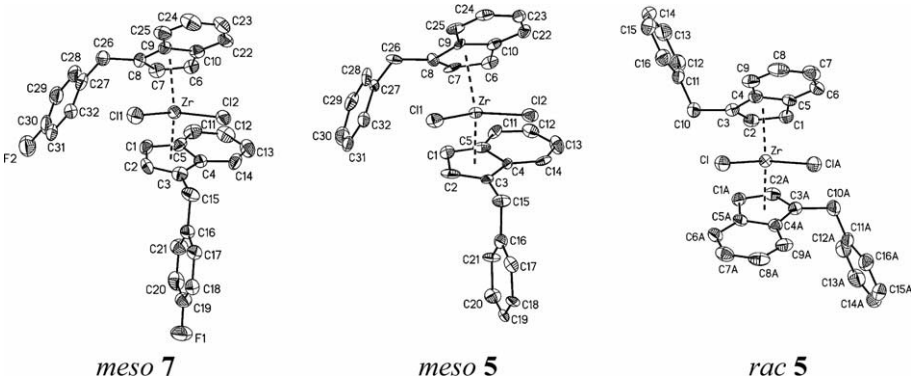

Fig. 1. Crystal structures of complexes *meso*-**7**, *meso*-**5** and *rac*-**5**.

Table 1
Selected bonding parameters for *rac*- and *meso*-**5**

Parameter	*meso*-**5**	*rac*-**5**
Zr–Cl1	2.417(3) Å	2.4358(12) Å
Zr–Cl2	2.431(4) Å	2.4358(12) Å
Zr–Cp1	2.223 Å	2.224 Å
Zr–Cp2	2.237 Å	2.224 Å
Cl1–Zr–Cl2	95.55(14)°	96.22(6)°
ϕ, Cp1–Zr–Cp2[a]	128.5°	128.1°
C15–Cp1–Cp2–C26[b]	78.2°	
C10–Cp1–Cp2–C10A[b]		0.0°
β, Cp1–Zr[c]	3.2	3.5°
β, Cp2–Zr[c]	5.6°	3.5°
θ[d]	55.2(6)°	58.9(1)°

Cp1 and Cp2 refer to the centers of the cyclopentadienyl ring plane.
[a] Bending angle.
[b] Dihedral angle.
[c] Deviation from perpendicularity to the Cp–Zr vector.
[d] Angle between the two Cp planes.

for Ind_2ZrCl_2 in the solid state [12]. Also the Cp1–Zr–Cp2 angle (*meso* 128.5° and *rac* 128.1°) correlates with the values for **7** (129.0), Ind_2ZrCl_2 (128.3°) and bis{(1-cyclohexyl)tetrahydroindenyl}$ZrCl_2$ (*meso* 130.5° and *rac* 130.8°) [9,11]. These values are typical for unbridged group 4 metallocenes, being a few degrees larger than those for the corresponding ethyl-bridged *ansa*-complexes [13]. The distances between zirconium and the Cp carbon atoms in *meso*-**5** vary from 2.417(11) to 2.631(11). The corresponding distances of *rac* **5** range from 2.469(4) to 2.594 Å, and can be considered as typical values for η^5:η^5 coordination distances for bent metallocenes. The angle between the two Cp planes, θ, is reduced in *meso*-**5**, as expected when indenyl is substituted in 1-position. The values of deviations from perpendicularity to the Zr–Cp vectors β are comparable to those of *meso*-**7**. In the crystal structure of *meso*-**5** the benzyl substituents point towards the same direction like in *meso*-**7** but the dihedral angle (C15–Cp1–Cp2–C26, 78.2°) is diminished from that of *meso*-**7**. In the structure of *rac*-**5** the corresponding dihedral angle is 0°, indicating that the benzyl substituents are oriented in opposite directions.

2.3. Ethene polymerization and characterization of polyethene

The catalytic behavior of **5**–**8** was studied in ethene polymerization at 50 °C at three different monomer pressures (2.8, 3.8 and 4.6 bar), after activation with MAO. The results are presented in Table 2. Both *meso* and *rac* forms of the catalysts were examined (except complex **8**) and generally the two isomers behaved differently. The dependence of the activity on the ethene pressure is presented in Fig. 2.

Rac and *meso*-**6**/MAO, having a MeO group in *para*-position were least active of the catalysts studied and their activity was almost pressure independent, while the molar mass of the polymers increased steadily with monomer pressure. The molar mass distribution, MMD, of the polymer produced with *meso*-**6**/MAO increases from 4.2 to 4.5 with the pressure. The *rac* form behaved differently; the molar mass distribution increased from 6.0 to 10.3 when pressure was raised from 2.8 to 4.6 bars.

Both *rac* and *meso* isomers of unsubstituted **5**/MAO were clearly more active than the corresponding isomers of **6**. The activity of *rac* **5**/MAO was almost independent of pressure, 25–29 $kg_{PE}/mmol_{cat}$ h, while the activity of *meso*-**5**/MAO increased from 13 to 41 $kg_{PE}/mmol_{cat}$ h. The molar mass of the polymers made with the *meso*-**5**/MAO increased up to pressure of 3.8 bar and then it stayed constant. In the same pressure range the molar mass of the polymers prepared with the corresponding *rac* form increased from 480 to 700 kg/mol. With both *meso* and *rac* forms, molar mass distributions were maximum at pressure of 3.8 bar.

Both isomers of the *para*-fluoro-substituted catalyst **7**/MAO were the most active in the series of the benzyl–indenyl zirconium dichlorides. Activity increased with pressure for both *meso* and *rac* catalyst: with the *meso* form from 21 to 55 $kg_{PE}/mmol_{cat}$ h and the *rac* form 39 to 47 $kg_{PE}/mmol_{cat}$ h. The molar mass of the polymers produced with *rac*- and *meso*-**7**/MAO increased with ethene pressure: *rac*-**7**/MAO from 475 to

Table 2
Ethene polymerization results with *rac* and*meso* isomers of catalysts **5**–**8**/MAO[a]

Catalyst	Pressure (bar)	Activity ($kgPE/mmol_{cat}$ h)	M_w (kg/mol)	M_n (kg/mol)		MWD	T_m (°C)	Vinyl%	*trans*-Vinylene%	Vinylidene%
			GPC	GPC	FT-IR	(M_w/M_n)	DSC	FT-IR	FT-IR	FT-IR
rac-**5**	2.8	29.0	487.2	169.2	189.0	2.88	133.7	83.9	11.8	4.3
rac-**5**	3.8	25.2	629.8	185.9	200.6	3.39	133.8	86.3	9.6	4.1
rac-**5**	4.6	26.7	710.3	223.4	226.7	3.18	133.5	91.3	5.0	3.7
meso-**5**	2.8	12.8	586.2	207.1	233.1	2.83	134.0	87.7	8.1	4.1
meso-**5**	3.8	31.4	680.5	182.4	213.3	3.73	133.3	86.9	8.8	4.3
meso-**5**	4.6	40.7	677.6	218.5	266.0	3.10	135.5	85.8	12.5	1.6
rac-**6**	2.8	18.3	442.8	73.80	57.33	6.00	134.0	93.8	4.4	1.8
rac-**6**	3.8	17.2	465.8	53.23	45.11	8.75	134.0	96.4	2.1	1.4
rac-**6**	4.6	16.0	539.2	52.60	47.22	10.25	135.0	96.6	2.0	1.4
meso-**6**	2.8	8.0	229.8	54.79	39.52	4.19	133.3	96.2	2.0	1.8
meso-**6**	3.8	8.4	240.3	53.99	39.99	4.45	134.4	97.0	1.4	1.6
meso-**6**	4.6	8.9	270.4	52.60	43.60	4.54	135.0	97.4	0.75	1.8
rac-**7**	2.8	39.2	487.9	167.9	130.9	2.92	133.5	86.4	10.6	2.9
rac-**7**	3.8	39.2	608.6	169.7	124.0	3.59	134.8	89.5	7.2	3.3
rac-**7**	4.6	46.8	724.5	156.1	144.3	4.64	134.1	90.4	7.8	2.0
meso-**7**	2.8	20.8	456.3	156.5	150.0	2.92	133.9	87.4	9.5	3.1
meso-**7**	3.8	38.0	558.2	203.5	196.2	2.74	133.0	87.4	9.4	3.2
meso-**7**	4.6	55.0	606.8	222.7	201.1	2.73	133.9	88.2	8.1	3.8
rac-**8**	2.8	105.6	471.0	242.8	292.1	1.94	135.7	86.9	10.2	2.9
rac-**8**	3.8	178.7	493.3	273.9	276.5	1.80	134.2	87.3	10.4	2.4
rac-**8**	4.6	205.7	444.7	249.8	268.0	1.78	134.7	90.0	6.9	3.1

[a] Polymerization conditions: ethene pressures: 2.8, 3.8 and 4.6 bar, reactor temperature 50 °C, Al:Zr = 9000 (*rac* and *meso* **5**–**7**), 27000 (*rac*-**8**), polymerization time ca. 30 min. Amount of catalyst: 0.3 μmol (*rac* and *meso* **5**–**7**), 0.1 μmol (*rac*-**8**).

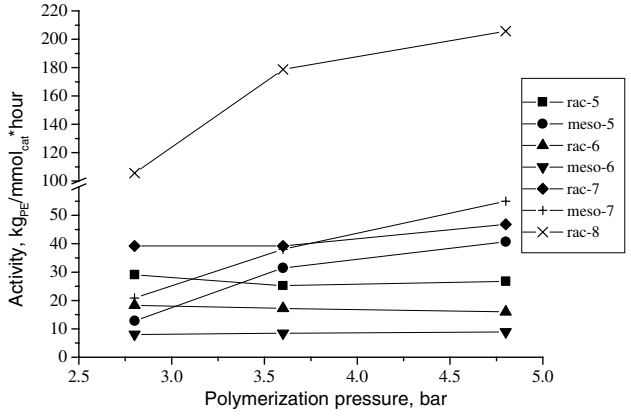

Fig. 2. Ethene polymerization activities of catalysts *rac* and *meso* **5**–**7**/MAO and *rac*-**8**/MAO.

700 kg/mol and *meso*-**7**/MAO from 450 to 600 kg/mol. In the related pressure range the MMD of the polyethene prepared with *meso*-**7**/MAO stayed almost constant at about 2.8 and with *rac*-**7**/MAO it increased from 2.8 to 4.5.

2.4. Correlation between the catalyst structures and the polymerization behavior

Ab initio calculations indicated that an intramolecular interaction between the benzyl moiety and zirconium center is relevant in cationic methyl complexes and the coordination of the benzyl ring to the metal center occurs from *o*-carbon as illustrated in Fig. 3. In general the coordination mode agrees with the earlier results of Saßmannshausen et al. [7] calculated for [(η^5-Cp)(η^5-$CpCH_2C_6H_5$)]$ZrMe^+$. The bond distances and intramolecular phenyl metal coordination energies are presented in Table 3. The coordination energies are estimated by presenting the stabilities of the coordinating isomers (*meso*-a and *rac*-c) relative to the corresponding non-coordinating *rac*-b isomers presented in Fig. 3. The metal–phenyl coordination energies are of the same magnitude with metal–ethene coordination energies, which in the case of the *rac*-b isomer of **5** are 55 and 53 kJ/mol by HF/3-21G$^{(*)}$ and B3LYP/6-31G* methods, respectively. The HF/3-21G$^{(*)}$ method somewhat overestimates both metal–phenyl coordination energies and Zr–C distances, but is capable of producing the stability trends (OMe > H > F) in line with B3LYP/6-31G* calculations. It should be noted that complexes are subject to basis-set superposition error. BSSE corrections, calculated by the counterpoise method, decrease the interaction energies by approximately 20 kJ/mol. The influence of BSSE is systematic, therefore not affecting the qualitative trends.

We assume that the phenyl–metal interaction is probably the main reason for of the low polymerization activity of the benzyl catalysts **5**–**7**/MAO; the coordination of the benzyl moiety to the vacant coordination site interferes the monomer coordination. In the

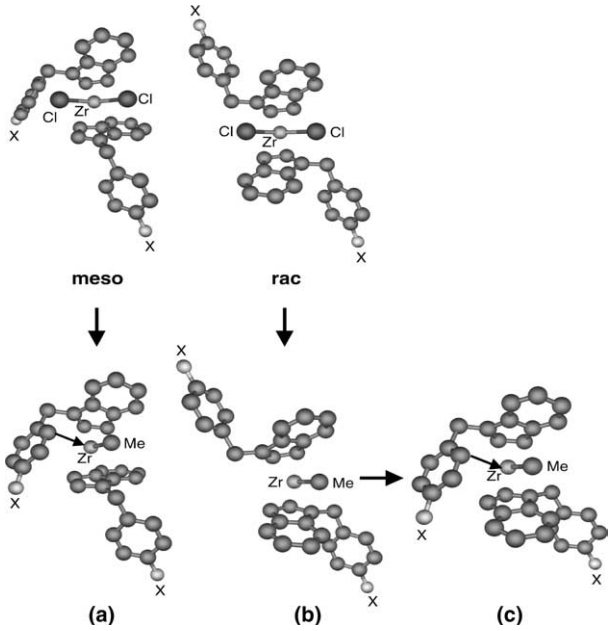

Fig. 3. Hartree–Fock optimized structures of dichloride and cationic monomethyl forms of studied benzyl-substituted {η^5-(1-benzyl)indenyl}zirconocenes. (**5**) X = H; (**6**) X = OMe; (**7**) X = F.

Table 3
Calculated relative stabilities (ΔE; kJ/mol) of intramolecular benzyl coordination in the cationic monomethyl forms of the *rac* and *meso* isomers of **5**–**7** and closest Zr–C_{Ph} distances

Isomer	Substituent	HF/3-21G(*)		B3LYP/6-31G*	
		ΔE (kJ/mol)	Zr–C (Å)	ΔE (kJ/mol)	Zr–C_{Ph} (Å)
Rac-**5**a	H	−62	2.75	−52	2.71
Meso-**5**c	H	−62	2.76	−47	2.68
Rac-**6**a	OMe	−67	2.77	−52	2.73
Meso-**6**c	OMe	−70	2.73	−52	2.67
Rac-**7**a	F	−62	2.78	−50	2.71
Meso-**7**c	F	−55	2.76	−42	2.70

phenylethyl-substituted complex *rac*-**8**, the ethyl bridge elongates the distance between the phenyl ring and the Zr center and the coordination of phenyl is not energetically favorable because such a coordination would require the transformation of the carbon chain from *trans* to *gauche* conformation [7]. As a result, *rac*-**8**/MAO is much more active than the benzyl-substituted complexes studied in this work and acts like a typical single site metallocene catalyst producing polyethene with narrow molar mass distribution close to numeric value two. This finding is in accordance with Licht et al. [10c], who have shown that activity increases with chain length of the carbon spacer between the Cp moiety and the phenyl group.

The moderately active diastereomers of **5**/MAO and **7**/MAO produced high molar mass polyethene with slightly broadened molar mass distribution. High molar mass indicates decreased rate of chain termination, which may also explain the high *trans*-vinylene end group concentrations in polymers made with the catalysts (see below). The corresponding diastereomers of **5**/MAO and **7**/MAO follow same trends in activity, molar mass and polydispersity. The *meso* isomers of catalysts **5**/MAO and **7**/MAO were more responsive to increasing monomer pressure than the *rac* forms, which produce PE with rather constant activity regardless the applied monomer concentration (Fig. 2). The stronger coordination of the benzyl group in the *rac*-isomers could be an explanation for the observed polymerization behavior (Table 3).

According to the calculations, an electronegative *para*-fluoro substituent in the benzyl group in complex **7** decreases electron density in the phenyl ring and, weakens its interaction with the metal center (Table 3) and enhances the polymerization activity of *rac*- and *meso*-**7**/MAO compared to *rac*- or *meso*-**5**/MAO. Correspondingly the activities were lowest for the methoxy-substituted catalysts *rac*- and *meso*-**6**/MAO. This can be explained by the inductive effect of the electron-donating methoxy group which increases electron density in the phenyl ring and the attraction between the phenyl ring and the electron-deficient metal cation becomes stronger.

Molar mass distribution of the polymers prepared with *rac*- and *meso*-**6**/MAO are significantly broad (4.2–10.25) and this indicates the presence of several active species. According to the study of Piccolrovazzi et al. MAO has propensity to coordinate with MeO-groups in $[4,7\text{-}(MeO)_2Ind]_2ZrCl_2$ which cause broadening of the MMD. In addition, MAO coordination causes further congestion around the catalytic active metal center and leads to reduced activity. Besides the strong phenyl interaction, another reason for the low activity might be the coordination of Lewis-acidic aluminum centers of the MAO to the methoxy group [14]. Together with strong metal–phenyl interaction the above-mentioned coordination of MAO with MeO-groups offer a rational explanation for the observed polymerization behavior of *rac* and *meso* isomers of **6**/MAO.

2.5. Chain termination reactions

To have a deeper insight for the polymerization reaction, unsaturated chain end structures formed by chain termination reactions were measured by FT-IR. Absorbances of vinyl (908.8 cm^{-1}), vinylidene (888.2 cm^{-1}) and *trans*-vinylene (966 cm^{-1}) end groups were determined [15] and the corresponding calculated end group distributions are presented in Table 2. In general, number average molar mass, M_n, values obtained by FT-IR and GPC followed each other well for the polymers prepared at different pressures (Figs. 4 and 5) in spite that

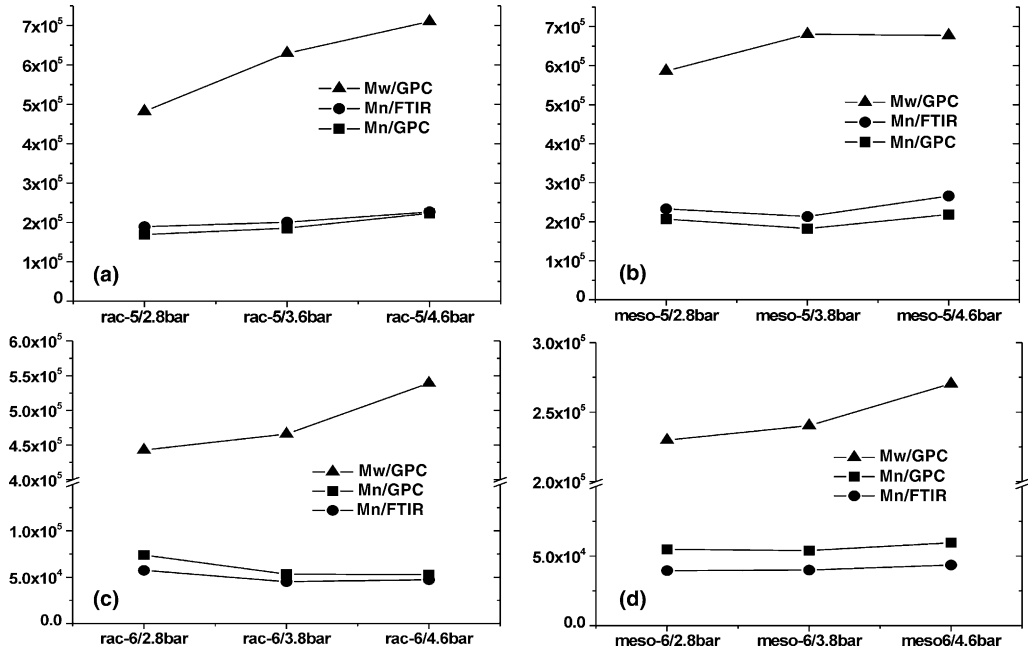

Fig. 4. Weight average molar mass, M_w, and number average molar mass, M_n, obtained with GPC and FT-IR of the polyethenes prepared in pressures of 2.8, 3.8 and 4.6 bar with catalysts **5**/MAO: *rac* (a) and *meso* (b) and catalyst **6**/MAO: *rac* (c) and *meso* (d).

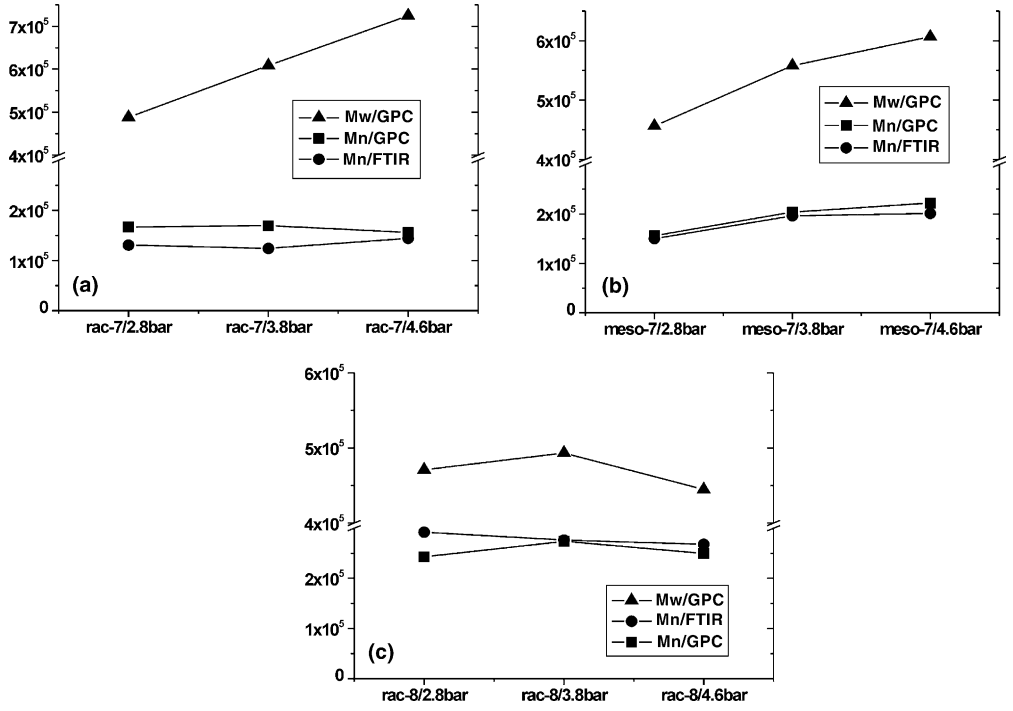

Fig. 5. Weight average molar mass, M_w, and number average molar mass, M_n, obtained with GPC and FT-IR of the polyethenes prepared in pressures of 2.8, 3.8 and 4.6 bar with catalysts **7**/MAO: *rac* (a) and *meso* (b) and catalyst **8**/MAO: *rac* (c).

the difference between these two values was substantial in many cases.

With catalyst *meso*-**5**/MAO the M_n values calculated from FT-IR data are systematically higher than results from GPC data (Fig. 4(b)). This indicates the presence of saturated end groups in the polymers probably formed by the termination via chain transfer to the cocatalyst [16]. Similar observations were made for polyethenes synthesized with the catalysts **7**/MAO and **8**/MAO and correlations between M_n values obtained

by FT-IR and GPC are presented in Fig. 5. In polyethenes made with *meso*-**6**/MAO the difference between values obtained by FT-IR and GPC was almost constant and M_n-values obtained by FT-IR were systematically lower than those obtained by GPC (Fig. 5(b)). This is probably a result of the formation of internal double bonds to polymer chains by an allylic activation mechanism [17].

According to the theoretical calculations of Zielger et al. [18] thermodynamically favorable chain termination path in olefin polymerizations with metallocene catalysts is the β-hydride transfer to a coordinated monomer. This process leads to a vinyl chain end group to the polymer. An alternating chain termination mechanism, which leads also to formation of vinyl chain ends is intramolecular β-hydride elimination [20]. In all polyethenes of this study the vinyl end group was dominantly most common and its abundance varied from 86% to 97% of total amount of the unsaturated end groups.

The steric and electronic properties of the catalysts as well as polymerization conditions affect on the activation energies of the different termination reactions and can vary the ratio of the different end groups in the synthesized polymers. When the activation energy barrier for chain isomerization reaction is close to the β-hydride transfer, the probability to the chain termination via chain isomerization is increased. This termination reaction leads to a formation of *trans*-vinylene chain end groups and it is strongly affected by the steric properties of the catalyst [19]. Relatively high contents of *trans*-vinylene groups were detected in polyethenes prepared with both isomers of the catalysts **5**/MAO and **7**/MAO and *rac*-**8**/MAO the percentage of *trans*-vinylenes varied from 5.0% to 11.8% while in polymers made with both *rac*- and *meso*-**6**/MAO *trans*-vinylene contents only 0.8–4.4%. Decreased free space around the active sites of *rac*- and *meso*-**6** caused by the tightly coordinating benzyl substituent hinders rearrangement of the coordinated polymer and prevents formation of the *bis*-β-agostic structure, which is an essential intermediate in the chain isomerization process.

Vinylidene end groups in polyethenes have been explained in terms of the long chain branching mechanism. In situ formed polyethene macromonomers with a vinylic double bond at the chain end can make a reinsertion to the growing polymer [21]. If β-hydride transfer takes place after a 1,2-insertion of the macromonomer, a vinylidene end group is formed. Contents of vinylidene end groups were very low in all polymers (1.4–4.3%) and *rac* and *meso* isomers of **6**/MAO produced polymers with lowest content of vinylidene groups.

With increasing monomer pressure catalyst *rac*-**5**/MAO produced polymers with higher molar mass and vinyl content and lower amount of *trans*-vinylene chain ends. This illustrates that β-H elimination is an important chain termination reaction at higher monomer concentrations. The observations above and the fact that the activity of the *rac*-**5** did not increase at higher monomer concentrations are indications of the substantial benzyl coordination. On the contrary the molar mass of the polyethene prepared with *meso*-**5**/MAO was almost constant with increasing monomer concentration and the activity was clearly enhanced. As the amount of vinyl end groups was decreased and *trans*-vinylene end groups were increased, the termination reactions with *meso*-**5** were dominantly β-H transfer to a coordinated monomer and chain isomerization. Similar trends can be observed also for *rac*- and *meso*-**7**/MAO, while with the catalyst **6**/MAO the presence of several active species complicates the interpretation of the results.

3. Conclusions

Despite the freely rotating indenyl ligands, the *rac* and *meso* isomers of studied metallocenes had different polymerization properties and by changing the *para*-substituents the catalytic behavior of **5**–**7**/MAO can be fine tuned. Computational results of methylated cationic *rac* and *meso* isomers of complexes **5**–**7** showed that the benzyl substituent has a possibility for coordination with the cationic zirconium center. This coordination orientates the phenyl moiety against the metal center in all *rac* and *meso* benzyl–indenyl complexes. Calculations show a η^1-coordination between the metal and an *o*-carbon of the phenyl ring and the intramolecular coordination energies are of the same magnitude as of the ethene monomer. This creates a steric block to the incoming monomer, disturbs the coordination equilibrium, and creates catalytic centers with different properties as shown in the broadening of MMD. According to the polymerization results the overall polymerization activity was decreased but the molar mass of the polyethenes remained high. In *rac*-**8**/MAO, the interaction of the phenyl ring does not have a notable role in polymerization due to the elongated distance between metal and phenyl ring created by the ethyl spacer. Catalyst *rac*-**8**/MAO was significantly more active than the other catalysts and had a typical single-site polymerization character producing polyethene with polydispersity close to 2.0. All the catalysts produced polyethenes with predominantly vinyl end groups and the competing chain isomerization termination process produced ca. 10% of *trans*-vinylene units to the polymers (with the exceptions of the isomers of **6**/MAO).

3.1. General methods and materials

All reactions were carried out under argon atmosphere using standard Schlenk techniques. Diethyl ether, toluene, and hexane were purified by distillation on

sodium. Dichloromethane was distilled from CaH_2. The cocatalyst, methylaluminumoxane, MAO, 30 wt% solution in toluene, was received from Borealis Polymers. Compounds **7**–**8** were prepared according to the procedures presented in the literature [9,10].

3.2. Polymerization procedure

Polymerizations were performed in a thermostatic 1000 mL Büchi glass autoclave. The autoclave was loaded with 300 mL of toluene and required amount of 30% MAO in toluene. After this ethene was fed to the autoclave until saturated ethene/toluene solution was achieved. A constant ethene pressure was maintained with an automated pressure controller. The polymerizations were started by injecting 20 mL of zirconocene dichloride precursor solutions into the autoclave. Ethene consumption was monitored by a flow controller connected to a computer. The polymerizations were stopped by unloading the autoclave of the ethene and leading the polymerization solutions to HCl–methanol solutions. The precipitated polymers were washed with methanol, filtered and dried overnight at 60 °C.

In the polymerizations with both isomers of the catalysts **5**, **6** and **7** the amount of catalyst was 0.3 μmol and the calculated Al:Zr was 9000. With highly active catalyst, *rac*-**8**/MAO, only 0.1 μmol of the catalyst was used in order to hold the polymerization process controllable. As the same amount of MAO was added in all the polymerizations to utilize stable scavenging effect of free TMA, the Al:Zr ratio with catalyst *rac*-**8**/MAO was 27 000.

3.3. Polyethene characterization

Molar mass and molar mass distributions were measured with a Polymer Labs high temperature GPC apparatus equipped with refractive index and light scattering detectors. Chromatographic runs were performed at 140 °C with 1,2,4-trichlorobenzene as an eluent; the flow rate was kept at 1.0 mL/min. Absolute M_w values were computed from data of a 15° and 90° light scattering detector.

End group analysis of polyethenes was done with a Perkin–Elmer Fourier transform infrared spectrometer. The spectra were measured from thin disks prepared from polyethenes. PE sample powder (0.2 g) was pressed onto a film at ambient temperature between two smooth steel plates using a hydraulic press. A round disk of 13 mm of diameter was cut from the film and its thickness, approximately 0.50 mm, was measured with a micrometer. The disk was placed into the IR sample holder and measured with 16 scans from 4000 to 370 cm^{-1} with 0.5 cm^{-1} nominal resolution. Baseline correction of the absorbance spectrum was done by an interactive method. Corrected absorbance values of the vinylidene peak at 888 cm^{-1}, the vinyl peak at 908 cm^{-1} and the *trans*-vinylene peak at 966 cm^{-1} were used to calculate the concentrations of the corresponding terminal groups [15].

Melting temperatures were measured with a Perkin–Elmer DSC-2 equipped with a digital data acquisition device. Thermogramms were measured from 30 to 230 °C using a temperature scanning rate of 10 K/min. Peak melting temperature was determined from the second heating curve.

3.4. Computational details

All geometry optimizations were carried out with the GAUSSIAN 03 program package [22], using HF/3-21G$^{(*)}$ and hybrid density functional B3LYP/6-31G* methods [23]. Since the standard 6-31G* basis set is not available for zirconium, Zr was described by Huzinaga's extra basis (Zr, 433321/433/421) [24]. Theoretical treatment of transition metal complexes generally requires the use of more sophisticated methods than Hartree–Fock, mainly due to near-degeneracy and relativistic effects [25]. However, zirconium is located at the beginning of the second transition row in the periodic table, which means that near-degeneracy and relativistic effects are weak and the Hartree–Fock method at the HF/3-21G$^{(*)}$ level is capable of predicting the structures of zirconocenes with a considerable accuracy. This was recently demonstrated with a set of 62 zirconocenes characterized by crystallographic method in which the crystal structures were compared with the corresponding optimized structures [26]. Furthermore, the performance of the HF/3-21G$^{(*)}$ method was found to be comparable or superior to the more expensive no local density functional BLYP [27], hybrid density functional B3LYP and MP2 calculations with larger basis sets.

3.5. Synthesis of complexes

3.5.1. (1-Benzyl)indene (*1*)

n-Butyllithium (1.6 M in hexane, 26.6 ml, 42.6 mmol) was added dropwise at 0 °C to a solution of indene (5 ml, 42.6 mmol) and Et_2O and the reaction was completed by the addition of benzyl bromide (5.0 ml, 42.6 mmol). After stirring overnight at ambient temperature, an aqueous solution of NH_4Cl was added and the mixture was extracted with Et_2O. The solvent was evaporated and the crude products were purified by column chromatography giving yellow oils.

1 (Crude product 7.2 g, 35.0 mmol, 82%) MS(EI) *m*/*z* HRMS(EI) Calcd. for C_{16} H_{14}. Found: ^{1}H NMR (200 MHz, $CDCl_3$) $\delta = 2.63$ (dd, 1H, $J = 9.2/4.2/9.2$ Hz, CH_2), 3.04 (dd, 1H, $J = 6.8/6.8/6.8$ Hz, CH_2), 3.60–3.68 (m, 1H, CH_{Ind}), 6.36 (d, 1H, $J = 7.4$ Hz, CH_{Ind}), 6.72 (d, 1H, $J = 7.4$, CH_{Ind}), 7.09–7.31 (m, 9H, aromatic H). Anal. Calcd. for $C_{16}H_{14}$: C, 93.16; H, 6.84. Found: C, 90.43; H, 6.85%.

*3.5.2. 1-(p-Methoxy benzyl)indene (**2**)*

This ligand was prepared in the same way as **1** except that *para*-methoxy benzyl chloride (5.78 ml, 42.6 mmol) was added to the indenyl lithium.

2 (Crude product 8.0 g, 33.9 mmol, 80%) ^{1}H NMR (200 MHz, $CDCl_3$) δ = 2.58 (dd, 1H, J = 8.8/4.6/9.2 Hz, CH_2), 2.95 (dd, 1H, J = 7.0/6.6/7.0 Hz, CH_2), 3.55–3.82 (4H, CH_3 + CH_{Ind}), 6.35 (dd, 1H, J = 1.6/3.8/1.8 Hz, CH_{Ind}), 6.68–7.27 (m, 9H, CH_{Ind} + aromatic H). Anal. Calcd. for $C_{17}H_{16}O$: C, 86.40; H, 6.83; O, 6.77. Found: C, 85.16; H, 6.82%. MS(EI) *m/z*: 236 (M^+).

*3.5.3. 1-(p-Fluoro benzyl)indene (**3**)*

The ligand was prepared according to the literature [14].

*3.5.4. 1-(Phenyl ethyl)indene (**4**)*

This ligand was obtained in the same manner as compound **1** except for the addition of 2-phenyl ethyl bromide (5.8 ml, 42.6 mmol) indenyl lithium salt.

4 (Crude product 6.8 g, 31.0 mmol, 75%) ^{1}H NMR (200 MHz, $CDCl_3$) δ = 1.66–1.84 (m, 1H, CH_2), 2.00–2.23 (m, 1H, CH_2), 2.54–2.62 (m, 2H, CH_2), 3.36–3.46 (m, 1H, CH_{Ind}), 6.48 (dd, 1H, J = 1.8/4.0/1.8 Hz, CH_{Ind}), 6.74 (d, 1H, J = 1.8/3.8/1.8 Hz, CH_{Ind}), 7.01–7.35 (m, 9H, aromatic H). Anal. Calcd. for $C_{17}H_{16}$: C, 92.68; H, 7.32. Found: C, 85.28; H, 6.88%.

*3.5.5. Bis(1-benzyl)indenylzirconium dichloride (**5**)*

The ligand **1** precursor (5.0 g, 24.2 mmol) was converted to a lithio salt by using *n*-butyllithium (15.2 ml, 24.2 mmol) at 0 °C in Et_2O. The reaction mixture was stirred 2 h at room temperature. After removal of the solvent the solid residue was cooled down to −78 °C. Cooled CH_2Cl_2 was added, followed by an addition of $ZrCl_4$ (3.1 g, 13.3 mmol). The reaction mixture was allowed to come to room temperature and stirred overnight. After filtering through Celite the solvent was distilled off and the solid residue was extracted with hot hexane and toluene. *meso* and *rac* isomers crystallized from the mother liquors, *meso* from toluene and *rac* from hexane.

5 (Crude product 5.5 g, 9.6 mmol, 79.0%) Anal. Calcd. for $C_{32}H_{26}ZrCl_2$: C, 67.11; H, 4.58. Found: C, 66.53; H, 4.68%.

rac-**5** ^{1}H NMR (200 MHz, $CDCl_3$) δ = 4.15 (q, 4H, J = 8.2/7.4/16.0 Hz, CH_2), 5.84 (d, 2H, J = 3.4 Hz, CH_{Ind}), 6.07 (d, 2H, J = 3.0 Hz, CH_{Ind}), 7.12–7.67 (m, 18H, aromatic H). ^{13}C NMR, CCl3D: 140.0 (C, C-11), 128.9 (CH, C-13,15), 128.7 (CH, C-12,16), 127.0–126.4 (CH, C-6,7), 126.2–125.8 (CH, C-5,8), 124.0 (CH, C-14), 99.3 (CH, C-2,3), 52.0 (C, C-1), 34.2 (CH2, C-10).

meso-**5** ^{1}H NMR (200 MHz, $CDCl_3$) δ = 4.18 (q, 4H, J = 7.2/15.6/11.0 Hz, CH_2), 5.31 (d, 2H, J = 4.0 Hz, CH_{Ind}), 6.31 (d, 2H, J = 3.0 Hz, CH_{Ins}), 7.12–7.67 (m, 18H, aromatic H). 13C NMR, CCl3D: δ, 139.7 (C, C-11), 129.1 (CH, C-13,15), 128.8 (CH, C-12,16), 126.4, 126.3 (CH, C-6,7), 125.5 (CH, C-5,8), 123.7 (CH, C-14), 99.4 (CH, C-2,3), 70.8 (C, C-1), 30.0 (CH2, C-10).

*3.5.6. Bis{(1-p-methoxy benzyl)indenyl}zirconium dichloride (**6**)*

The methoxy-substituted complex was prepared in a similar manner to complex **5** (ligand **2** 5.7 g, 24.2 mmol). The *rac* isomer was obtained from toluene extraction and the *meso* isomer from hexane extraction.

6 (Crude product 5.8 g, 9.2 mmol, 76%) Anal. Calcd. for $C_{34}H_{30}O_2ZrCl_2$: C, 64.54; H, 4.78; O, 5.06. Found: C, 64.34; H, 4.85%. MS(EI) *m/z*: 632–636 (M^+), 397 ($M^+ - 2$).

rac-**6** ^{1}H NMR (200 MHz, $CDCl_3$) δ = 3.69 (d, 6H, J = 5.2 Hz, CH_3), 3.96 (s, 2H, CH_2), 4.06 (s, 2H, CH_2), 5.73 (d, 2H, J = 3.0 Hz, CH_{Ind}), 5.97 (d, 2H, J = 3.2 Hz, CH_{Ind}), 6.69–6.73 (m, 3H, aromatic H), 6.96–7.25 (m, 10H, aromatic H), 7.49–7.56 (m, 3H, aromatic H). ^{13}C NMR, CCl3D: δ, 158.3 (C, C-14), 132.0 (C, C-11), 129.9 (CH, C-12,17) 126.8–126.2 (CH, C-6,7), 125.8–125.5 (CH, C-5,8), 114.1 (CH, C-13,16) 99.3 (CH, C-2,3), 70.8 (C, C-1), 55.4 (CH3, C-15), 33.3 (CH2, C-10).

meso-**6** ^{1}H NMR (200 MHz, $CDCl_3$) δ = 3.70 (d, 6H, J = 5.2 Hz, CH_3), 4.10 (d, 4H, J = 3.2 Hz, CH_2), 5.22 (d, 2H, J = 2.8 Hz, CH_{Ind}), 6.20 (d, 2H, J = 3.0 Hz, CH_{Ind}), 6.74–6.79 (m, 3H, aromatic H), 7.05–7.33 (m, 10H, aromatic H), 7.54–7.57 (m, 3H, aromatic H). ^{13}C NMR, CCl3D: δ, 158.4 (C, C-14), 131.6 (C, C-11), 130.1 (CH, C-12,17), 126.6–126.0 (CH, C-6,7), 126.0–125.2 (CH, C-5,8), 114.1 (CH, C-13,16), 99.2 (CH, C-2,3), 55.4 (CH3, C-15), 33.4 (CH2, C-10).

*3.5.7. Bis{(1-phenyl ethyl)indenyl}zirconium dichloride (**8**)*

This complex was prepared in the same way as complex **5** (ligand 5.3 g, 24.2 mmol). The *rac* isomer was obtained from the toluene mother liquor.

8 (Crude product 5.7 g, 9.5 mmol, 78%) Anal. Calcd. for $C_{34}H_{30}ZrCl_2$: C, 67.98; H, 5.03. Found: C, 66.16; H, 5.02%.

rac-**8** ^{1}H NMR (200 MHz, $CDCl_3$) δ = 2.67–3.20 (m, 8H, CH_2), 5.74 (d, 2H, J = 2.4 Hz, CH_{Ind}), 5.85 (d, 2H, J = 2.6 Hz, CH_{Ind}), 6.98–7.59 (m, 18H, aromatic H). ^{13}C NMR (CCl3D): δ, 141.5 (C, C-12), 128.7 (CH, C-14,16), 128.5 (CH, C-13,17), 126.0–126.8 (CH, C-6,7), 125.5–126.0 (CH, C-5,8), 99.1 (CH, C-2,3), 70.8 (C, C-1), 36.1 (CH2, C-11), 30.1 (CH2, C-10).

3.6. X-ray crystallographic studies

The crystal data of *meso*-**5** and *rac*-**5** were collected on a Rigaku AFC-7S single crystal diffractometer at

193(2) K using Mo Kα radiation (graphite monochromatized, scan type $w/2\theta$). Intensities were corrected for Lorentz and polarization effects and for absorption (0.89 < 1.00). Solution: Direct methods combined with subsequent Fourier analysis. All non-hydrogen atoms were refined anisotropically. Hydrogen atoms were refined isotropically on calculated positions (riding model). Suitable crystals for X-ray determination were obtained by recrystallization. The *meso* isomer crystallized from hot hexane and the *rac* crystals from hot toluene. Calculations were carried out with SHELXTL/PC and SHELSL-93 programs.

meso: Crystal dimensions $0.15 \times 0.15 \times 0.08$ mm, $a = 10.380(4)$, $b = 11.715(4)$, $c = 20.972(6)$, $\alpha = \beta = \gamma = 90°$, $V = 2550.2(15)$ Å^3, crystal system orthorhombic, space group $P2(1)2(1)2(1)$, $Z = 4$, D(calcd) = 1.491 g/cm^3, $\lambda = 0.71073$ Å, data collection range $\theta = 2.61$–$24.99°$, reflections collected 2144, independent reflections 2144, reflections refined 1418, goodness-of-fit on $F^2 = 0.994$, $R_1 = 0.0695$ and $wR_2 = 0.0804$ (with $I_0 > 2\delta I_0$), $R_1 = 0.1171$ and $wR_2 = 0.909$ (all data). The largest difference peak and hole in the final residual electron density map is situated in the vicinity of zirconium (0.477 and −0.558 e Å^{-3}).

rac: Crystal dimensions $0.70 \times 0.25 \times 0.08$ mm, $a = 19.559(4)$, $b = 6.6980(10)$, $c = 20.551(4)$ Å, $\alpha = \gamma = 90°$, $\beta = 107.76(3)°$, $V = 2564.0(8)$ Å^3, crystal system monoclinic, space group $C2/c$, $Z = 4$, D(calcd) = 1.483 g/cm^3, $\lambda = 0.71073$ Å, data collection range $\theta = 2.52$–$22.49°$, reflections collected 2872, independent reflections 1628, reflections refined 1367, goodness-of-fit on $F^2 = 1.015$, $R_1 = 0.0397$ and $wR_2 = 0.0918$ ($I_0 > 2\delta I_0$), $R_1 = 0.0524$ and $wR_2 = 0.0962$ (all data). The largest difference peak and hole in the final residual electron density map is situated in the vicinity of zirconium (0.441 and −0.604 e Å^{-3}).

4. Supplementary material

Crystallographic data for the structural analyses of the complexes have been deposited with Cambridge Crystallographic Data Centre, CCDC, No. 222747 for *rac*-**5** and 222746 for *meso*-**5**. Copies of this information is available free of charge from: CCDC, 12 union Road, Cambridge CB2 1EZ, UK; fax: +44-123-336-336033; e-mail: deposit@ccdc.cam.ac.uk.

Acknowledgments

Finnish Technology Development Center (TEKES) and Academy of Finland (projects 204408 and 77317) are acknowledged for funding of the research. Hedvig Byman-Fagerholm is thanked for her expert assistance in the FT-IR measurements.

References

[1] (a) L. Resconi, L. Cavallo, A. Fait, F. Piemontesi, Chem. Rev. 100 (2000) 1253;
(b) H.H. Brintzinger, D. Fischer, R. Mülhaupt, B. Rieger, R.M. Waymouth, Angew. Chem., Int. Ed. Engl. 34 (1995) 1143;
(c) G.W. Coates, Chem. Rev. 100 (2000) 1223.
[2] H. Yiannoulakis, A. Yiagopoulos, P. Pladis, C. Kiparissides, Macromolecules 33 (2000) 2757.
[3] W. Kaminsky, Macromol. Chem. Phys. 197 (1996) 3907.
[4] (a) P.C. Möhring, N.J. Coville, J. Organomet. Chem. 479 (1994) 1;
(b) H.G. Alt, A. Köppl, Chem. Rev. 100 (2000) 1205, see also [1].
[5] M. Bochmann, M.L.H. Green, A.K. Powell, J. Saßmannshausen, M.U. Triller, S. Wocadlo, J. Chem. Soc., Dalton Trans. (1999) 43.
[6] L. Doerrer, M.L.H. Green, D. Häußinger, J. Saßmannshausen, J. Chem. Soc., Dalton Trans. (1999) 2111.
[7] M. Bühl, J. Saßmannshausen, J. Chem. Soc., Dalton Trans. (2000) 79.
[8] Diastereomers of unbridged 1-substituted metallocenes should be denoted as *rac*-like and *meso*-like. Further in the text they are denoted simply as *rac* and *meso* which is a common practice in the referred papers.
[9] G. Jany, M. Gustafsson, T. Repo, E. Aitola, J.A. Dobado, M. Klinga, M. Leskelä, J. Organomet. Chem. 553 (1998) 173.
[10] (a) N.E. Grimmer, N.J. Coville, C.B. de Koning, J.M. Smith, L.M. Cook, J. Organomet. Chem. 616 (2000) 112;
(b) N.E. Grimmer, N.J. Coville, C.B. de Koning, J. Organomet. Chem. 642 (2002) 195;
(c) E.H. Licht, H.G. Alt, M.M. Karim, J. Organomet. Chem. 599 (2000) 261;
(d) E.H. Licht, H.G. Alt, M.M. Karim, J. Organomet. Chem. 599 (2000) 275.
[11] (a) G. Erker, M. Aulbach, M. Knickmeier, D. Wingbermühle, C. Krüger, M. Nolte, S. Werner, J. Am. Chem. Soc. 115 (1993) 4590;
(b) C. Krüger, F. Lutz, M. Nolte, G. Erker, M. Aulbach, J. Organomet. Chem. 452 (1993) 79.
[12] T. Repo, M. Klinga, I. Mutikainen, Y. Su, M. Leskelä, M. Polamo, Acta Chem. Scand. 50 (1996) 1116.
[13] (a) S. Collins, B.A. Kuntz, N.J. Taylor, D.G. Ward, J. Organomet. Chem. 342 (1988) 21;
(b) W. Kaminsky, K. Kuelper, H.H. Brintzinger, F.R.W.B. Wild, Angew. Chem. 97 (1985) 507.
[14] (a) N. Piccolrovazzi, P. Pino, G. Consiglio, A. Sironi, M. Moret, Organometallics 9 (1990) 3098;
(b) M. Linnolahti, T.A. Pakkanen, Macromolecules 33 (2000) 9205;
(c) P. Foster, M.D. Rausch, J.C.W. Chien, J. Organomet. Chem. 527 (1997) 71.
[15] J. Haslam, H.A. Willis, D.C.M. Squirrel, Identification and Analysis of Plastics, second ed., Illiffe Books, London, 1972.
[16] (a) L. Resconi, S. Bossi, L. Abis, Macromolecules 23 (1990) 4489;
(b) L. Resconi, F. Piemontesi, G. Franciscono, L. Abis, T. Fiorani, J. Am. Chem. Soc. 114 (1992) 1025;
(c) S. Lieber, H.H. Brintzinger, Macromolecules 33 (2000) 9192.
[17] G. Moscardi, L. Resconi, Organometallics 20 (2001) 1918.
[18] J.C.W. Lorenz, T.K. Woo, L. Fan, T. Ziegler, J. Organomet. Chem. 449 (1995) 91.
[19] (a) V. Busico, R. Cipullo, J. Am. Chem. Soc. 116 (1994) 9329;
(b) K. Thosrhaug, J.A. Støvneng, E. Rytter, M. Ystenes, Macromolecules 31 (1998) 7149;
(c) P. Lehmus, E. Kokko, R. Leino, H. Luttikhedde, B. Rieger, J.V. Seppälä, Macromolecules 33 (2000) 8534;
(d) M.K. Leclerc, H.H. Brintzinger, J. Am. Chem. Soc. 118 (1996) 9024.

[20] (a) M.H. Prosenc, H.H. Brintzinger, Organometallics 16 (1997) 3889;
(b) P.M. Margl, T.K. Woo, T. Ziegler, Organometallics 17 (1998) 4997.
[21] (a) A. Malmberg, J. Liimatta, A. Lehtinen, B. Löfgren, Macromolecules 32 (1999) 6689;
(b) T.K. Woo, P.M. Margl, T. Ziegler, Organometallics 16 (1997) 3454.
[22] M.J. Frisch, G.W. Trucks, H.B. Schlegel, G.E. Scuseria, M.A. Robb, J.R. Cheeseman, J.A. Montgomery, T. Vreven, Jr., K.N. Kudin, J.C. Burant, J.M. Millam, S.S. Iyengar, J. Tomasi, V. Barone, B. Mennucci, M. Cossi, G. Scalmani, N. Rega, G.A. Petersson, H. Nakatsuji, M. Hada, M. Ehara, K. Toyota, R. Fukuda, J. Hasegawa, M. Ishida, T. Nakajima, Y. Honda, O. Kitao, H. Nakai, M. Klene, X. Li, J.E. Knox, H.P. Hratchian, J.B. Cross, C. Adamo, J. Jaramillo, R. Gomperts, R.E. Stratmann, O. Yazyev, A.J. Austin, R. Cammi, C. Pomelli, J.W. Ochterski, P.Y. Ayala, K. Morokuma, G.A. Voth, P. Salvador, J.J. Dannenberg, V.G. Zakrzewski, S. Dapprich, A.D. Daniels, M.C. Strain, O. Farkas, D.K. Malick, A.D. Rabuck, K. Raghavachari, J.B. Foresman, J.V. Ortiz, Q. Cui, A.G. Baboul, S. Clifford, J. Cioslowski, B.B. Stefanov, G. Liu, A. Liashenko, P. Piskorz, I. Komaromi, R.L. Martin, D.J. Fox, T. Keith, M.A. Al-Laham, C.Y. Peng, A. Nanayakkara, M. Challacombe, P.M.W. Gill, B. Johnson, W. Chen, M.W. Wong, C. Gonzalez, J.A. Pople, Gaussian Inc., Pittsburgh, PA, 2003.
[23] C. Lee, W. Yang, R.G. Parr, Phys. Rev. B 37 (1988) 785.
[24] S. Huzinaga, Gaussian Basis Sets for Molecular Calculations, Elsevier, Amsterdam, 1984.
[25] (a) P.E.M Siegbahn, Adv. Chem. Phys. 93 (1996) 333;
(b) P. Pyykkö, Chem. Rev. 88 (1988) 563.
[26] M. Linnolahti, P. Hirva, T.A. Pakkanen, J. Comput. Chem. 22 (2001) 51.
[27] D. Becke, Phys. Rev. A 38 (1988) 3098.